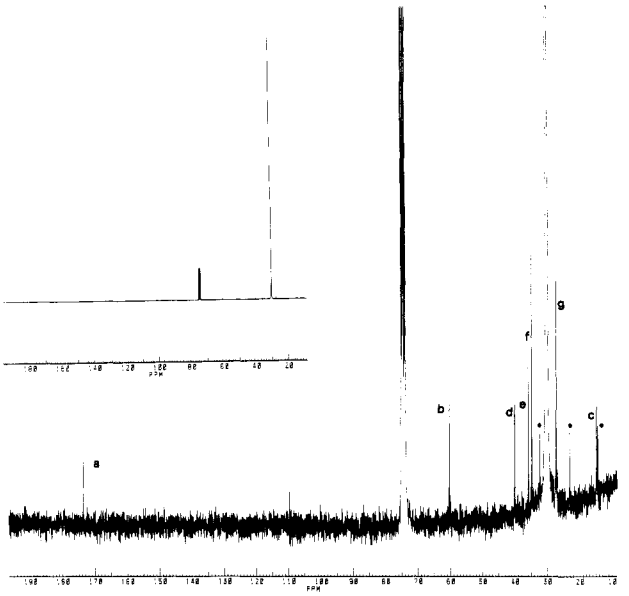

Figure 1. ^{13}C NMR spectrum of high-density polyethylene functionalized with ethyl diazoacetate. The insert shows the same spectrum reduced 256 times. Letters are referred in Table I; asterisks show heptane impurity.

5 by each side) inserted between them and the g carbons.

Indeed the asymmetric model **1b** shows chemical shifts of d–g closer to those of the corresponding C atoms in the polymer than **1a**; similarities are enhanced by considering, successively, the d–g carbon atoms.

The chemical shifts of the d atom in **1a** and **1b** are similar, with that of **1b** slightly closer to the FHDPE chemical shift. Differences between the **1a** and **1b** spectra become more consistent when considering the e–g peaks; in particular, the last two assignments approximate very well the f and g FHDPE chemical shifts.

In the FHDPE spectrum (Figure 1) peaks are also observed (marked with an asterisk) attributable to *n*-heptane used for performing extractions of the functionalized polymer; the evaluated concentration of *n*-heptane in FHDPE is <0.1% w/w, showing the dramatic potentialities of ^{13}C NMR spectroscopy to detect impurities at very low concentrations.

The observed similarities among the spectra of FHDPE and of the low molecular weight models **1a** and **1b** strongly support the idea that the functional groups attached to the HDPE chain by thermal decomposition of EDA are in fact $-CH_2COOEt$ groups, as expected from the carbene mechanism shown in Scheme I.

In this sense, ^{13}C NMR spectroscopy has been shown to be a very powerful tool, allowing us to detect carbonyl groups, which are really "dispersed" to very low concentration (approximately 0.3–0.4% w/w with respect to the polymer) in the aliphatic moiety. The most important conclusion from the present work, however, is the demonstration of the possibility of performing a clean chemical modification on a paraffinic macromolecule.

It is worth mentioning that structure **3** corresponds to that of a linear copolymer of ethylene with ethyl 1-butenoate, which up to now has not even been prepared by direct copolymerization.

Experimental Section

Ethyl (3-butyl)heptanoate (**1a**) was obtained in 40% yield by reacting 5-bromononane (5.39 g, 2.6×10^{-2} mol; **2a**) with an ethanol solution of sodium diethylmalonate (2.61×10^{-2} mol) according to literature methods,[5] subsequently, the initially formed product was saponified and decarboxylated at 180 °C for 3 h. The crude acid obtained (2.5 g) was esterified with "super dry" ethanol (17 mL) and a catalytic amount of concentrated sulfuric acid (1 mL), by refluxing the mixture over 20 h. The final product **1a** was isolated by distillation under reduced pressure (2.15 g, 1×10^{-2} mol); bp 115–125 °C (23 mmHg), in good agreement with literature data.[6] It was characterized by ^1H NMR and ^{13}C NMR spectroscopy. ^1H NMR (in $CDCl_3$, TMS): δ 4.13 (q, 2 H), $-OCH_2CH_3$), 2.23 (d, 2 H, $-CHCH_2COOEt$), 1.85 (br m, 1 H, $-CHCH_2COOEt$), 1.26 (m, 15 H, aliphatic CH_2 + OCH_2CH_3), 0.89 (t, 6 H, CH_3). ^{13}C NMR: see Table I.

Ethyl (3-pentyl)undecanoate (**1b**) is not described in the literature; it was obtained in 41% yield by the procedure described above for the synthesis of **1a**. **1b** was characterized by elemental analysis (Calcd: C, 75.99; H, 12.75. Found: C, 74.96; H, 12.72) and by ^1H NMR and ^{13}C NMR spectroscopy. ^1H NMR (in $CDCl_3$): δ 4.12 (q, 2 H, $-OCH_2CH_3$), 2.22 (d, 2 H, $-CHCH_2COOEt$), 1.85 (br m, 1 H, $-CHCH_2COOEt$), 1.26 (m, 25 H, aliphatic CH_2 + OCH_2CH_3), 0.89 (t, 6 H, CH_3). ^{13}C NMR: see Table I.

HDPE was functionalized by reacting the polymer with EDA by the procedure described in ref 3. ^{13}C NMR spectra of FHDPE were run in 1,2-dideuteriotetrachloroethane solutions (200 mg/3 mL) at 110 °C, 10-mm NMR tube. A total of 40 000 scans, with 45° pulses and a relaxation time of 5 s, was necessary in order to obtain the spectrum shown in Figure 1.

Due to the low content of functionalized units special care was paid to the signal to noise ratio. Thus, the Ernst angle[7] was used with an approximate T_s obtained by considering the NMR experiments on low-density polyethylenes.[8,9]

The quantitative analysis was performed by comparing the intensities of peaks g and f (belonging to the main chain near branches) with the polyethylene peaks, on the reasonable hypothesis of equal NOE's for all the backbone carbon atoms. Assignments, shown in Table I were made by additivity rules.[10] The ^{13}C NMR spectra of model compounds were run in $CDCl_3$ at room temperature in 10% by volume solutions, on a Varian VXR-300 spectrometer operating at 75.4 MHz.

Registry No. **1a**, 80256-56-0; **1b**, 117801-00-0; HDPE, 9002-88-4.

References and Notes

(1) Ruggeri, G.; Aglietto, M.; Petragnani, A.; Ciardelli, F. *Eur. Polym. J.* **1983**, *19*, 863.
(2) Von E. Doering, W.; Knox, L. H. *J. Am. Chem. Soc.* **1956**, *78*, 4947; **1961**, *83*, 1989.
(3) Demonceau, A.; Noels, A. F.; Hubert, A. J.; Teyssié, P. 2nd IUPAC Symposium on Organometallic Chemistry Directed toward Organic Synthesis, Dijon, France, 1983.
(4) Skell, P. S.; Aglietto, M.; Ruggeri, G.; Speranza, S.; Ciardelli, F. Italian Patent 48950A/85, 1985.
(5) *Vogel's Textbook of Practical Organic Chemistry*, 4th ed.; Longman: London, 1978.
(6) Malthete, J.; Canceill, J.; Gabard, J.; Jacques, J. *Tetrahedron* **1981**, *37*, 2823.
(7) Ernst, R. R.; Bodenhausen, G.; Wokaun, A. *Principles of NMR in One and Two Dimensions*; Oxford Science Publications: 1987; p 125.
(8) Axelson, D. E.; Levy, G. C.; Mandelkern, L. *Macromolecules* **1979**, *12*, 41.
(9) Cavagna, F. *Macromolecules* **1981**, *14*, 215.
(10) Stothers, J. B. *Carbon-13 Spectroscopy*; Academic Press: New York, 1972.

Gas Permeability of a Polystyrene/Polybutadiene Block Copolymer Possessing a Misoriented Lamellar Morphology

J. CSERNICA, R. F. BADDOUR, and R. E. COHEN*

Department of Chemical Engineering, Massachusetts Institute of Technology, Cambridge, Massachusetts 02139.
Received August 8, 1988;
Revised Manuscript Received October 7, 1988

Introduction

In an earlier paper,[1] the gas permeability of a polybutadiene/polystyrene block copolymer with highly oriented lamellar domains was investigated. The mor-

0024-9297/89/2222-1493$01.50/0

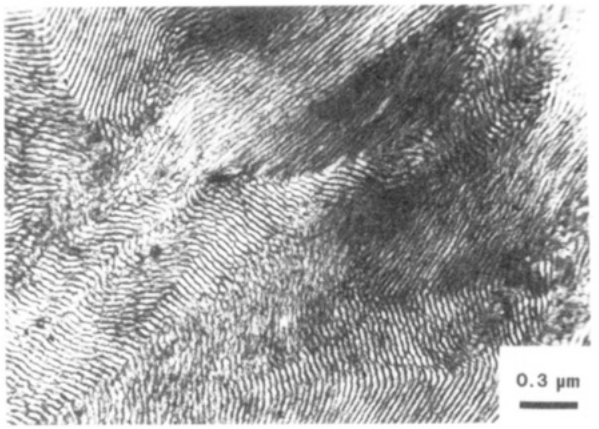

Figure 1. Transmission electron micrograph displaying cross-sectional view of KR-ST sample film.

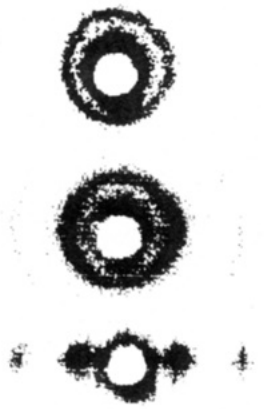

Figure 2. Small-angle X-ray scattering patterns for (a, top) KR-ST with beam perpendicular to film surface and (b, middle) KR-ST with beam parallel to film surface. (c, bottom) Pattern for the same block copolymer whose domains are highly ordered.[1] The first-order maxima occur at $Q = 0.015$ Å^{-1}.

phologies of many heterogeneous polymer systems, however, are not well aligned or ordered but possess overall isotropy. Here we propose a simple model to describe gas transport in one example of this type of polymer—a block copolymer possessing a misoriented lamellar morphology.

Experimental Section

The polymer used in this study was the same K-Resin block copolymer used in our previous work.[1] Films of 0.5–0.7 mm were cast from 5% solutions in toluene by solvent evaporation over 6 days on a flat Teflon surface at 40 °C in an enclosed chamber with nitrogen gas sweep. These samples were then annealed under vacuum for 24 h at 110 °C. Samples of this type are designated KR-ST (for "K-Resin: static cast").

Transmission electron microscopy (TEM) of osmium-stained sections from sample films revealed the expected lamellar morphology.[1] As seen in Figure 1, there exist distinct grains of approximately 1000–10 000 Å in size, within which the lamellae arrange themselves parallel to one another. The direction of orientation varies from one grain to the next in a seemingly random fashion, which indicates the lack of long-range order. Interestingly, the polybutadiene and polystyrene domains are seen to be continuous across the grain boundaries even when the orientation direction changes drastically. This demonstrates the strong thermodynamic tendency for unbroken lamellae to form for this system.

In order to obtain a more global view of sample morphology, small-angle X-ray scattering patterns with the beam both parallel and perpendicular to the film surface have been collected (Figure 2). These also indicate little or no overall preferred alignment of domains. (For comparison, a SAXS pattern for the previously studied block copolymer sample with long-range order[1] is also shown.) It is concluded that these static cast samples KR-ST can be considered macroscopically isotropic.

Table I
Experimental and Predicted Permeability Coefficients[a]

	P				
	Ar	Kr	N_2	CO_2	CH_4
Experimental					
PB	55	117	21	435	83
PS	1.6	0.7	0.6	13	0.8
KR-ST	5.1	7.0	2.1	45	5.9
Predictions					
Sax and Ottino	8.8	14.6	3.3	70	11
random column (2 phase)	6.7	9.0	2.4	52	7.2
random column w/interphase	5.7	7.2	2.1	46	5.8

[a] Permeability in 10^{-10} (cm^3 (STP) cm)/(cm^2 s cmHg).

Results and Discussion

Permeability coefficients for various gases in these films were measured by using a variable volume permeability apparatus.[1,2] Results are presented in Table I, along with permeability values for polystyrene (PS) and polybutadiene (PB) homopolymers.

Sax and Ottino[3,4] have developed a model for gas diffusion in a two-phase lamellar system possessing "small-scale order and large-scale disorder". This description fits the morphology of our samples. The system was modeled[3] as a large-scale random medium consisting of many distinct, well-ordered lamellar units. Each of these morphological units is described by three principal axes (1, 2, and 3)—two which view lamellar regions in parallel and one which does so in series. Expressions for the diffusion coefficient in each direction were presented. Based on a scheme which statistically averages diffusion through these units over all possible orientations, the effective or overall diffusion coefficient for the system was given[3,4] as the average of the diffusion coefficients (D) in the principal directions:

$$D_{\text{eff}} = (1/3)(D_1 + D_2 + D_3) \tag{1}$$

It is straightforward to extend their model from diffusion to permeability coefficients by multiplying the diffusion coefficients (D_1, D_2, and D_3) by a solubility coefficient (S_{total}) for a two-phase system:[5]

$$S_{\text{total}} = S_{\text{B}}\upsilon_{\text{B}} + S_{\text{S}}\upsilon_{\text{S}} \tag{2}$$

where S_{B}, S_{S} = solubility coefficient for polybutadiene, polystyrene and υ_{B}, υ_{S} = volume fraction of polybutadiene, polystyrene. The resulting expressions for the permeability coefficient for each axis of the basic morphological unit reduce to the permeability models for parallel (axes 2 and 3) and series (axis 1) laminates:[6]

$$P_{\text{par}} = P_{\text{B}}\upsilon_{\text{B}} + P_{\text{S}}\upsilon_{\text{S}} \tag{3}$$

$$P_{\text{ser}} = P_{\text{B}}P_{\text{S}}/(P_{\text{B}}\upsilon_{\text{S}} + P_{\text{S}}\upsilon_{\text{B}}) \tag{4}$$

where P_{B}, P_{S} = permeability coefficient for polybutadiene, polystyrene.

With this extension from diffusion to permeability coefficients, the result of Sax and Ottino gives the effective P for the system:

$$P_{\text{eff}} = (1/3)(P_{\text{ser}} + P_{\text{par}} + P_{\text{par}}) \tag{5}$$

The first row of numbers below the experimental permeabilities in Table I represents predictions for the effective permeability coefficient from the above model as applied to the present system. It is evident that the model overpredicts (by as much as a factor of 2) the values de-

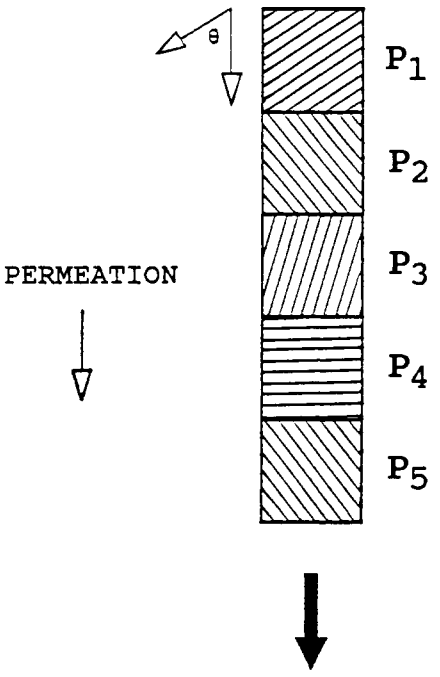

Figure 3. Random column representation.

termined experimentally here for the KR-ST samples.

It is believed that this disagreement results from the manner in which the series and parallel modes of permeation are combined in the Sax and Ottino model. The arithmetic averaging in eq 5 implies that the series and parallel laws are effectively combined *in parallel*. This type of formulation would apply to a physical condition where two-thirds of the permeating molecules encounters a completely parallel morphological situation and one-third of the molecules experiences a totally series situation. In reality, however, it is likely that *every* diffusing molecule which travels through the collection of randomly oriented grains will undergo some of its transport in the slower series mode. As a result, the total flux through the material will be greatly inhibited as compared to the situation described by eq 5.

As an alternative to this averaging scheme, a different model is proposed here which we have termed the "random column model". The morphology of the sample is modeled as columns of cubical cells, with each column extending directly from one surface of the film to the other. A two-dimensional representation of such a column appears in Figure 3. Each cell contains alternating parallel lamellae which possess a direction of orientation defined by a random angle θ.

The present model assumes that the permeating species will preferentially diffuse parallel to the lamellar orientation in each cell—in effect following its "path of least resistance". A periodic boundary condition is imposed at the left and right sides of the cell so that any gas that "leaves" through either side of the cell as it travels parallel to the orientation direction reenters at the opposing side. With these considerations, the permeability for each cell can be defined as the permeability for a parallel lamellar system, divided by a path length or tortuosity factor τ, which will change from cell to cell:

$$P_i = P_{par}/\tau_i \tag{6}$$

This tortuosity factor accounts for the fact that a lamellar alignment angle θ (Figure 3) other than zero increases the path length a diffusing molecule must travel in order to reach the cell below. The tortuosity factor for any cell can be expressed as

$$\tau_i = 1/(\cos\theta_i) \tag{7}$$

The model must also recognize that a cell's permeability coefficient will never be lower than that given by the series representation (eq 4). To account for this, if the tortuosity for a cell is so large that the permeability calculated by P_{par}/τ_i is lower than that from the series model, the series value is assigned as the permeability for that cell. In effect, the diffusing species is allowed to "choose" the faster of the two modes (series versus parallel) through any cell.

Once every cell in the column has been assigned a permeability coefficient, these are combined *in series* to obtain the effective permeability for the entire column:

$$1/P_{eff} = (1/N)(1/P_1 + 1/P_2 + 1/P_3 + ...) \tag{8}$$

where N = number of cells in the column.

A computer simulation of the random column in order to calculate effective column permeabilities has been carried out. Based on grain sizes observed from TEM, there are estimated to be 1000 cells (or grains) per column for our samples. As simulations were studied for our system, it became apparent that a column which contained this many cells behaved as if it possessed an infinite number of them. As a result, every column that comprises the sample will have an identical predicted permeability, and a single column result will be equal to the effective permeability for the entire film.

Since the building blocks of the random column model are results from series and parallel laws, it is a simple matter to incorporate the concept of the contribution of the interphase region[1] into the model. Both the series and parallel laws can be modified to consider a thrid component—the interphase region—and these new results can be used in the random column formulation. The three-phase series (P_{ser3}) and parallel (P_{par3}) permeabilities are given by

$$1/P_{ser3} = \Phi_S/P_S + \Phi_B/P_B + \Phi_I/\bar{P}_I \tag{9}$$

$$P_{par3} = \Phi_S P_S + \Phi_B P_B + \Phi_I \bar{P}_I \tag{10}$$

where subscript I's refer to the interfacial region, Φ is volume fraction, and $\bar{P}_I$ is the average permeability of the interphase.[1] The volume fractions for this block copolymer were reported in our previous investigation[1]

$$\Phi_{PS} = 0.63 \qquad \Phi_{PB} = 0.13 \qquad \Phi_I = 0.24 \tag{11}$$

Random column model predictions (with and without inclusion of the interfacial region) appear along with experimental data and results from the Sax and Ottino model in Table I. Predictions made using the random column model are superior to those calculated from the earlier model, and the agreement between model and experiment becomes excellent when the contribution of the interphase is considered.

The fact that the model works well for a series of gases, whose ratios of polybutadiene to polystyrene permeabilities range from 4 to over 150, convincingly demonstrates its ability to simulate the behavior of these block copolymer samples. Despite the simplifying assumptions involved, the random column model appears to have captured the essence of transport in this particular type of macroscopically isotropic system, and incorporation of further complications is unnecessary. It should serve as a useful predictive model for permeation in other heterogeneous systems with similar misordered morphologies.

Registry No. Ar, 7440-37-1; Kr, 7439-90-9; N_2, 7727-37-9; CO_2, 124-38-9; CH_4, 74-82-8; (B)(S) (block copolymer), 106107-54-4.

References and Notes

(1) Csernica, J.; Baddour, R. F.; Cohen, R. E. *Macromolecules* **1987**, *20*, 2468.

(2) *ASTM D-1434*; American Society for Testing and Materials: Philadelphia, 1984.
(3) Sax, J.; Ottino, J. M. *Polym. Eng. Sci.* **1983**, *23*(3), 165.
(4) Kinning, D. J.; Thomas, E. L.; Ottino, J. M. *Macromolecules* **1987**, *20*, 1129.
(5) Petropoulos, J. H. *J. Polym. Sci., Polym. Phys. Ed.* **1985**, *23*, 1309.
(6) Hopfenberg, H. B.; Paul, D. R. In *Polymer Blends*; Paul, D. R., Newman, S., Eds.; Academic: New York, 1978; Vol. 1, Chapter 10.

Surface Tension of Mixtures of Rodlike Particles: Monomer Effects

RANDALL S. FROST

1045 Catalina Drive, Apartment 13, Livermore, California 94550. *Received June 23, 1988; Revised Manuscript Received September 12, 1988*

The surface tension of an anisotropic monolayer was recently evaluated for athermal mixtures in which the solute comprises rodlike molecules having the familiar Flory distribution of axial ratios.[1] Reconsideration of the calculations in ref 1 has shown that the manner in which the surface tension function

$$H(x) = \left[\frac{v_1^{l} v_2^{l}}{v_2^{l} + v_1^{l}/x}\right]\{1 - 1/x - (y-1) \times (v_{2a}^{l}/x_{na}^{l} v_2^{l}) - (x_{nr}^{l} - 1)(v_{2r}^{l}/x_{nr}^{l} v_2^{l})\}$$

was previously evaluated overweighted the contribution from monomer present in the anisotropic phase. Correction for this problem suggests that the disordered monomer in the anisotropic phase may play a significant role in lowering surface tension. Here, as before, v_1 and v_2 are the volume fractions of solvent and solute in the liquid (superscript l), y is a disorder parameter whose generality is believed to exceed the limitations of the lattice model, and v_{2r}, v_{2a}, x_{nr}, and x_{na} represent the solute volume fractions and number average; axial ratios, x, correspond to randomly oriented (subscript r) and ordered (subscript a) solute species in the anisotropic phase, respectively. As previously defined,[1] when H is positive, the isotropic phase has a lower surface tension than the anisotropic phase, and when H is negative, the anisotropic phase has the lower surface tension.

Consider Figure 1, where H has been reevaluated as a function of the relative volume of isotropic phase ϕ for two values of x, $x = 1$ and $x = x_n^0 = 8$. Although there is still the rapid variation in H in the vicinity of $\phi = 0.99$, noted previously for the case $x = x_n^0 = 8$, two important effects can now be seen that did not show up before. The first is that H is positive for this value of x over the entire range of ϕ for which biphasic equilibria exists; the second is that H is 1 order of magnitude larger than previously calculated. The significance is that, for this value of x, the surface tension of the anisotropic phase will never be lower than that of the coexisting isotropic phase. Other observations, i.e., that H vanishes at the limits $\phi \approx 0.224$ and $\phi = 1.0$ and that the effect of increasing x from 8 to infinity on the behavior and magnitude of H is relatively small, continue to be valid.

We next consider H as a function of ϕ for $x = 1$, corresponding to a disordered monomer component within the anisotropic phase.[2] From Figure 1 it is seen that although the absolute magnitude of H is small, the function changes sign at $\phi \approx 0.7$. The change in sign of H turns out to be a consequence of y crossing the $y = 1$ boundary.

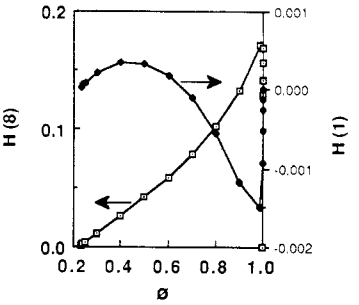

Figure 1. Surface tension function $H(x)$ representing self-ordering effects in an anisotropic monolayer that is in equilibrium with a biphasic solution of rigid rods for a most probable (Flory) distribution of axial ratios having $x_n^0 = 8$. The function has been evaluated at two axial ratios, $x = 1$ and $x = 8$. Note: When $H < 0$, the anisotropic phase has the lower surface tension, and when $H > 0$, the surface tension of the isotropic phase is lower. Although not apparent in the figure, H actually vanishes at four values of ϕ for $x = 1$ (see text).

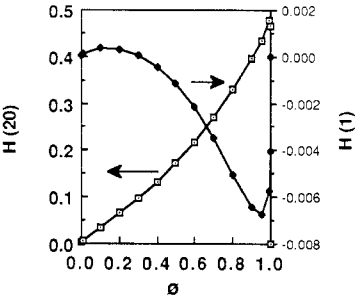

Figure 2. Surface tension function $H(x)$ for self-ordering for $x_n^0 = 20$ evaluated at $x = 1$ and at $x = 20$. Unlike the case of $x_n^0 = 8$, one can have biphasic equilibria for the mixture of rods for this value of x_n^0 when $\phi = 0$. The parameter H is small but greater than zero in this limit. Analysis shows that there are three values of ϕ for which H vanishes when $x = 1$, only two of which can be seen in the figure.

Analysis shows that the function remains negative for larger values of ϕ until $1 - \phi = 2.1 \times 10^{-8}$, where again $y = 1$ (see ref 2, p 1131). For larger values of ϕ, H is again positive. In the limit that $\phi = 1.0$, $H = 0$ as already noted. The fact that H is positive for ϕ very close to 1.0 means that the presence of monomer in the anisotropic surface layer cannot bring about a lowering of surface tension in this region. However, over the range of ϕ indicated, the disordered component ($x = 1$) of the anisotropic phase will have a lower surface tension than the bulk isotropic phase.

In Figure 2, H has been similarly recalculated as a function of ϕ for $x_n^0 = 20$, evaluated at $x = 1$ and at $x = x_n^0 = 20$. Although there is little qualitative difference seen in the behavior of H vs ϕ in Figures 1 and 2, there are two features of note: the range of H is now larger, and H now assumes negative values for $x = 1$ for ϕ as small as ~ 0.3. The surface tension of the monomer in the anisotropic phase is thus seen to be a stronger function of ϕ for the case $x_n^0 = 20$ than for $x_n^0 = 8$.

The behavior predicted for the case $\phi = 0$, corresponding to a completely anisotropic solution, also changes in light of the new calculations. Specifically, H is greater than or equal to zero for all species x. According to theory, the incipient isotropic phase will always have a surface tension that is lower or equal to that of the parent anisotropic phase.

References and Notes

(1) Frost, R. S. *Macromolecules* **1988**, *21*, 1854.
(2) Flory, P. J.; Frost, R. S. *Macromolecules* **1978**, *11*, 1126.

0024-9297/89/2222-1496$01.50/0